

GT2011-45( ' )

## AN ENERGY BASED CRITICAL FATIGUE LIFE PREDICTION METHOD

**Todd Letcher & M.-H. Herman Shen\***  
Department of Mechanical and Aerospace  
Engineering - The Ohio State University  
Columbus, OH, USA

**Onome Scott-Emuakpor, Tommy George &  
Charles Cross**  
Air Force Research Laboratory  
Dayton, OH, USA

### ABSTRACT

The capability of a critical life, energy-based fatigue prediction method is analyzed in this study. The theory behind the prediction method states that the strain energy accumulated during monotonic fracture and fatigue are equal. Therefore, a precise understanding of the strain energy density behavior in each failure process is necessary. The initial understanding of energy behavior shows that the accumulated strain energy density during monotonic fracture is the area underneath the experimental stress-strain curve, whereas the sum of the constant area within every stress-strain hysteresis loop of the cyclic loading process is the total strain energy density accumulated during fatigue; meaning, fatigue life is determined by dividing monotonic strain energy density by the strain energy density in one cycle. Further observation of the energy trend during fatigue shows that strain energy density per cycle is not constant throughout the process as initially assumed. This finding led to the incorporation of a critical life effect into the energy-based fatigue prediction method. The analysis of the method's capability was conducted on Al 6061-T6 ASTM standard specimens. The results of the analysis provide further improvement to the characterization of strain energy density for both monotonic fracture and fatigue; thus improving the capability of the energy-based fatigue life prediction method.

### NOMENCLATURE

$\beta_0$  - straight line material parameter  
 $\beta_1$  - straight line material parameter  
 $\varepsilon$  - true strain

$\varepsilon_0$  - material parameter for monotonic strain  
 $\varepsilon_f$  - true strain at fracture  
 $\varepsilon_n$  - true strain at necking  
 $\varepsilon_{pp}$  - peak to peak true strain  
 $\sigma$  - true stress  
 $\sigma_0$  - defined material parameter  
 $\sigma_a$  - amplitude of alternating stress  
 $\sigma_c$  - material parameter for cyclic strain  
 $\sigma_f$  - true stress at fracture  
 $\sigma_n$  - true stress at necking  
 $\sigma_{pp}$  - peak to peak true stress  
 $\sigma_y$  - true yield stress

A - scaling parameter for energy curve  
B - scaling parameter for energy curve  
C - cyclic strain scaling factor  
 $d_f$  - diameter after monotonic fracture  
E - modulus of elasticity  
N - number of cycles  
 $N_c$  - number of cycles to critical lifetime  
 $N_f$  - number of cycles to failure  
q - shape parameter for energy curve  
p - shape parameter for energy curve  
W - strain energy at a given point in lifetime  
 $W_{cycle}$  - strain energy accumulated per cycle  
 $W_{crit}$  - cumulative strain energy to critical point  
 $W_m$  - strain energy for monotonic tensile case  
 $W_{CF}$  - fracture energy - curve fit approximation  
 $W_{SL}$  - fracture energy - straight line approximation

\* Corresponding author. Tel.: +1-614-292-2280;  
E-mail address: shen.1@osu.edu (M.-H. Herman Shen)

## INTRODUCTION

Accurately predicting fatigue life is critical for preventing premature failure of gas turbine engine components and preventing catastrophic failure of the entire system. Therefore, design tools such as a stress versus cycle (S-N) curve, Goodman and modified Goodman diagrams have been widely used by gas turbine engine designers [1-3]. Construction of these design tools requires significant amounts of empirical data, which means a considerable amount of time is needed for High Cycle Fatigue (HCF) predictions. In order to reduce this time and expedite the generation of fatigue data by reducing the amount of testing necessary, the correlation between fatigue and energy has been studied.

Researchers began investigating the correlation between fatigue life and strain energy as early as the 1920s, when Jasper proposed that fatigue life is related to the stored energy density per cycle in a material [4]. Further advancement in the fatigue life and energy correlation came during the 1960s. In 1961, Enomoto stated that failure of a component occurs when the energy absorbed during cyclic loading accumulates to a total energy value [5]. In 1966, Stowell confirmed this idea by showing that the cyclic strain energy accumulation was equal to the total energy accumulated in a monotonic tension test [6]. This concept allowed a fatigue life prediction method to be developed based on the strain energy per fatigue cycle.

Following Stowell, Scott-Emuakpor et al. improved the energy-based method capability to determine fatigue during uniaxial, multiaxial and transverse shear loading [7, 8]. A key component to this improved method is the simplification that the strain energy density of each cycle in a fatigue process is equal. Work by Feltner et al. show that this is an oversimplification, and that strain energy density increases as loading cycles reach fatigue life [9]. Recent validation of the Feltner et al. findings has been conducted for axial and torsional shear loading [10, 11]. In each case, strain energy density per cycle was observed periodically throughout the entire fatigue process. From these observations, it was noted that the strain energy density decreased slightly from the constant level at around 90% of the expected fatigue life, and then the energy increased rapidly until failure. The understanding of this strain energy behavior was incorporated into the energy-based fatigue prediction method for critical life determination, which was estimated at 90% of the expected fatigue life [10].

This study thoroughly investigates the strain energy density trend during fatigue to further improve the critical life prediction capabilities of the energy-based method. Furthermore, a simplification to the calculation of empirical monotonic energy was addressed. This investigation is consistent with previous work directed towards improving and adding additional capabilities to the energy method for fatigue life assessment of materials, which can be applied to fatigue life assessment of gas turbine engine components.

## PREVIOUS RESEARCH SCOPE

The axial energy based fatigue lifetime prediction method used in this study is based on the analysis of the true stress - true strain relationships for monotonic and cyclic loading. Equation 1 describes the behavior of the true stress - true strain curve in a monotonic test prior to necking where Equation 2 defines  $\sigma_0$  [6]. After necking, Equation 3 approximates the true stress - true strain relationship [7]. An equation to model the behavior of the hysteresis loop is also needed (Equation 4). Equation 4 is based on a generalized coordinate system, which modifies the value of both axes so the ends of the hysteresis loop are at the origin and the maximum stress and strain [8]. This concept is shown in Figure 1.

$$\varepsilon = \frac{\sigma}{E} + \varepsilon_0 \sinh\left(\frac{\sigma}{\sigma_0}\right) \quad (1)$$

$$\sigma_0 = \frac{\sigma_f - \sigma_y}{\ln\left(\frac{\varepsilon_N}{0.002}\right)} \quad (2)$$

$$\sigma = \beta_0 + \beta_1 \varepsilon \quad (3)$$

$$\varepsilon_{pp} = \frac{\sigma_{PP}}{E} + \frac{1}{c} \sinh\left(\frac{\sigma_{PP}}{\sigma_C}\right) \quad (4)$$

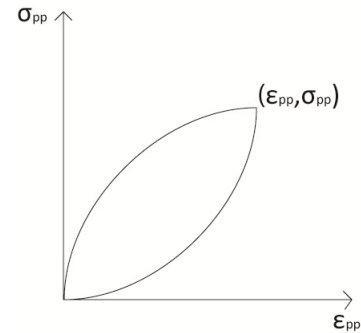


Figure 1. Hysteresis loop in generalized coordinates

This energy based fatigue life prediction framework, uses the total amount of strain energy to fracture a specimen during a monotonic test as the total strain energy to failure [7]. Equation 5 represents the strain energy in a monotonic test with the straight line assumption from necking to failure. The strain energy for a single fatigue cycle is calculated using Equation 6, which assumes the hysteresis loop is symmetric about a line drawn from the origin (0,0) to the maximum stress-strain point  $(\varepsilon_{pp}, \sigma_{pp})$ . This is a simplification that ignores the Bauschinger effect [12]. The integral in Equation 6 can be evaluated since we know the relationship for the strain in a cycle (Equation 4) in the generalized coordinate system. Equation 7 is the resulting relationship for strain energy per cycle when  $2\sigma_a$  is substituted for  $\sigma_{pp}$ . These relationships are then used to develop an equation for predicting fatigue life. The total strain energy in a monotonic

tension test is divided by the strain energy in one hysteresis loop to determine the expected lifetime as seen in Equation 8.

$$W_m = \sigma_n \left( \varepsilon_n - \frac{\sigma_n}{2E} \right) - \varepsilon_0 \sigma_0 \left[ \cosh \frac{\sigma_n}{\sigma_0} - 1 \right] + \frac{\beta_1}{2} (\varepsilon_f^2 - \varepsilon_n^2) + \beta_0 (\varepsilon_f - \varepsilon_n) \quad (5)$$

$$W_{cycle} = \sigma_{PP} \varepsilon_{PP} - 2 \int_0^{\sigma_{PP}} \varepsilon_{pp} d\sigma_{PP} \quad (6)$$

$$W_{cycle} = \frac{2\sigma_c}{c} \left[ \frac{\sigma_a}{\sigma_c} \sinh \left( \frac{2\sigma_a}{\sigma_c} \right) - \cosh \left( \frac{2\sigma_a}{\sigma_c} \right) + 1 \right] \quad (7)$$

$$N_f = \frac{\sigma_n \left( \varepsilon_n - \frac{\sigma_n}{2E} \right) - \varepsilon_0 \sigma_0 \left[ \cosh \frac{\sigma_n}{\sigma_0} - 1 \right] + \frac{\beta_1}{2} (\varepsilon_f^2 - \varepsilon_n^2) + \beta_0 (\varepsilon_f - \varepsilon_n)}{\frac{2\sigma_c}{c} \left[ \frac{\sigma_a}{\sigma_c} \sinh \left( \frac{2\sigma_a}{\sigma_c} \right) - \cosh \left( \frac{2\sigma_a}{\sigma_c} \right) + 1 \right]} \quad (8)$$

Since strain energy per cycle changes over the lifetime of specimens, it was important to address this trend in the prediction method [10, 13, 14, 16]. To observe the strain energy trend, a fatigue analysis showing strain energy density per cycle was conducted [15]. The result of this analysis, which is normalized with respect to the average strain energy density, is shown in Fig 2. The plot shows three specific trends for the strain energy density throughout the fatigue process. These trends are expressed by Eq. (9)-(11).

$$W(N) = Ae^{\frac{qN}{N_f}} \quad \text{for } 0 \leq N \leq 0.2N_f \quad (9)$$

$$W(N) = 1 \quad \text{for } 0.2N_f \leq N \leq 0.7N_f \quad (10)$$

$$W(N) = Be^{\frac{p(N-N_f)}{N_f}} \quad \text{for } 0.7N_f \leq N \leq N_f \quad (11)$$

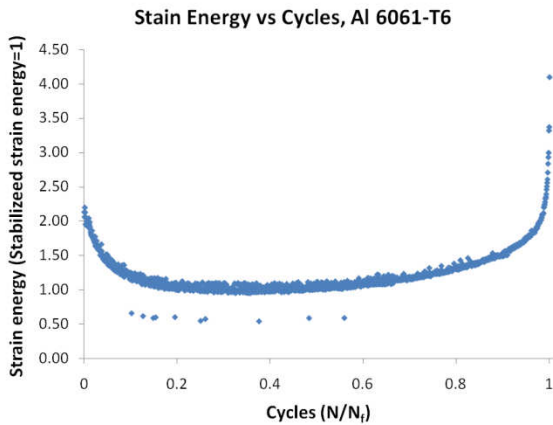


Figure 2. Strain energy variation over the lifetime of a specimen

Under the main assumption of this energy based fatigue lifetime prediction method, the energy accumulated over the

fatigue lifetime of the specimen is equal to the energy accumulated during a monotonic tensile test. Equation 12 is developed using the variable energy concept. This equation is then reduced to Equation 13, which predicts the lifetime of a specimen under a given fully reversed stress, where Equation 14 defines the constant D [15].

$$\left( \int_0^{0.2N_f} Ae^{\frac{qN}{N_f}} dN + \int_{0.2N_f}^{0.7N_f} 1 dN + \int_{0.7N_f}^{N_f} Be^{\frac{p(N-N_f)}{N_f}} dN \right) W_{cycle} = \sigma_n \left( \varepsilon_n - \frac{\sigma_n}{2E} \right) - \varepsilon_0 \sigma_0 \left[ \cosh \left( \frac{\sigma_n}{\sigma_0} \right) - 1 \right] + \beta_0 (\varepsilon_f - \varepsilon_n) + \frac{\beta_1}{2} (\varepsilon_f^2 - \varepsilon_n^2) \quad (12)$$

$$N_f = \left( \frac{1}{D} \right) C \frac{\sigma_n \left( \varepsilon_n - \frac{\sigma_n}{2E} \right) - \varepsilon_0 \sigma_0 \left[ \cosh \left( \frac{\sigma_n}{\sigma_0} \right) - 1 \right] + \beta_0 (\varepsilon_f - \varepsilon_n) + \frac{\beta_1}{2} (\varepsilon_f^2 - \varepsilon_n^2)}{\frac{2\sigma_c}{c} \left[ \frac{\sigma_a}{\sigma_c} \sinh \left( \frac{2\sigma_a}{\sigma_c} \right) - \cosh \left( \frac{2\sigma_a}{\sigma_c} \right) + 1 \right]} \quad (13)$$

$$D = \frac{A}{q} (e^{0.2q} - 1) + 0.5 + \frac{B}{p} (e^p - e^{0.7p}) \quad (14)$$

It has been previously estimated that the critical life of specimens is reached when the cumulative strain energy reaches about 90% of the strain energy accumulated in a monotonic test [10]. Developing a more rigorous understanding of these ideas and a more exact "critical lifetime" prediction is the focus of this study.

## EXPERIMENTAL PROCEDURES

The specimens used to conduct all of the tests were designed based on ASTM E466 [17]. Each specimen was machined according to Figure 3 from the same stock of Al6061-T6. The Al6061-T6 was received as cold finished, solution heat treated, quenched and artificially aged rods. The mechanical properties and heat treatment for this material are in accordance to AMS 2772 [18] and ASTM B211-03-M [19].

The testing was performed on an MTS load frame using semi-circular wedges and MTS model 647.10 hydraulic grips (see Figure 4). The specimens were gripped by the semi-circular wedges on the outer 38 mm; see the darkened areas of Figure 3. An MTS model 609.10A-01 alignment fixture was used to align the load frame. The load was measured by an MTS model 20E-03 load cell with a rated capacity of 100kN. Strain data were collected using an MTS axial extensometer, model 634.12E-24, with 14.66 mm gauge length. Data, such as time,

load, displacement and strain, were collected using an MTS TestStar IIs data acquisition system.

The accuracy of the extensometer was checked by comparing extensometer strain readings to a Micro-Measurements Division CEA-13-062UW-350 strain gauge. Figure 5 shows strain measurements for both techniques at 0.1 Hz and 207 MPa which shows the extensometer provided accurate results at this frequency and stress levels 207 MPa and above. Previous tests using the same load frame, controller, data acquisition system and extensometer also show a good comparison between the extensometer and Vishay CEA-13-062UW-350 strain gauges with a hysteresis loop - although on a flat specimen geometry [15]. The extensometer was necessary to obtain strain data throughout the entire lifetime on a single specimen, which would not have been possible to capture with a strain gauge due to low fatigue ratings for strain gauges. Previously, using strain gauges on multiple specimens to collect data for the entire lifetime of the specimen had been identified as a limitation [10, 11].

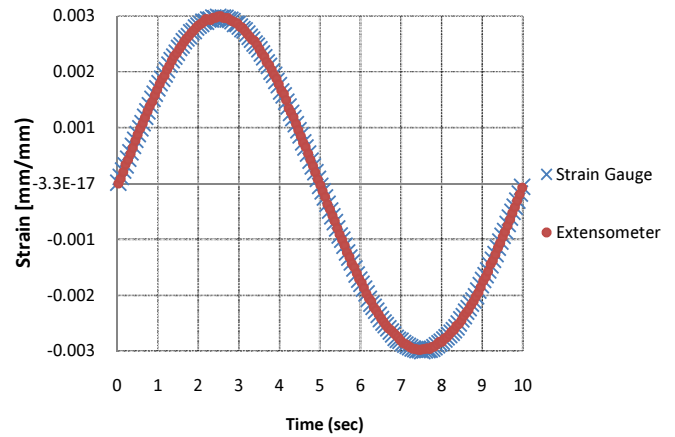


Figure 5. Strain gauge and extensometer comparison

Due to the slight variations in raw materials from stock to stock, all mechanical properties were tested for this stock of material and all values reported in this study are from this testing. In order to obtain these properties, monotonic tensile tests were conducted according to ASTM E8/E8M-08, Standard Test Methods for Tension Testing of Metallic Materials [20]. Specimens were displaced at a rate of 0.0254 mm/sec until the specimen completely fractured into two pieces with data collected at twenty data points per second. At the conclusion of the test, the fracture diameter was measured on both sides of the fractured specimen and averaged to determine the final fractured diameter.

In addition to testing for mechanical properties, an S-N curve for this particular stock of material was developed. The specimens were tested in load control at a load corresponding to the fully reversed stress level indicated. All S-N tests were conducted at 10 Hz using the sine tapered method of loading on the TestStar IIs controller to ensure the specimen did not experience stresses higher than specified [21].

Hysteresis data (force and strain) were collected throughout the specimen lifetime for several stress levels. These tests were preceded by a procedure necessary for determining the optimal testing frequency for reducing anelastic effects [10]. Since anelastic effects, such as damping and internal friction, have little or no effect on the microstructure of materials, the contribution of the effects to fatigue damage is insignificant [13]. Previous results from the optimal frequency determination procedure showed that 0.1 Hz was the fastest acceptable rate for testing and collecting only plastic strain energy [10]. Similar testing was conducted at 207MPa to determine the appropriate frequency rate to collect hysteresis data. Hysteresis data were collected between 0.001 Hz and 40 Hz. The perceived strain energy per cycle was highest at 40 Hz because anelastic effects dominated the strain measurements. The perceived strain energy decreased with decreases in testing frequency until reaching a steady value at 0.1 Hz. Because anelastic effects would affect perceived strain energy values above 0.1 Hz, all hysteresis data were collected at 0.1 Hz. See the complete results in Figure 6.

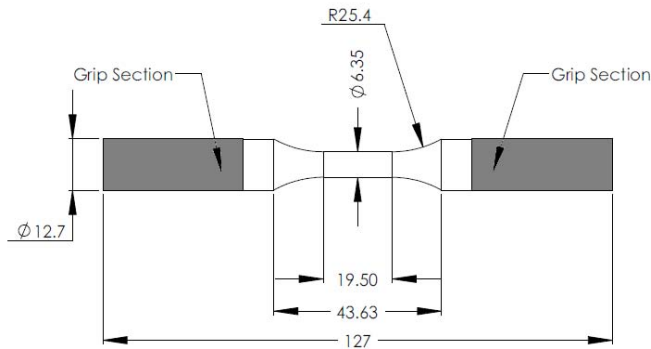


Figure 3. Specimen dimensions [mm]



Figure 4. MTS machine with extensometer

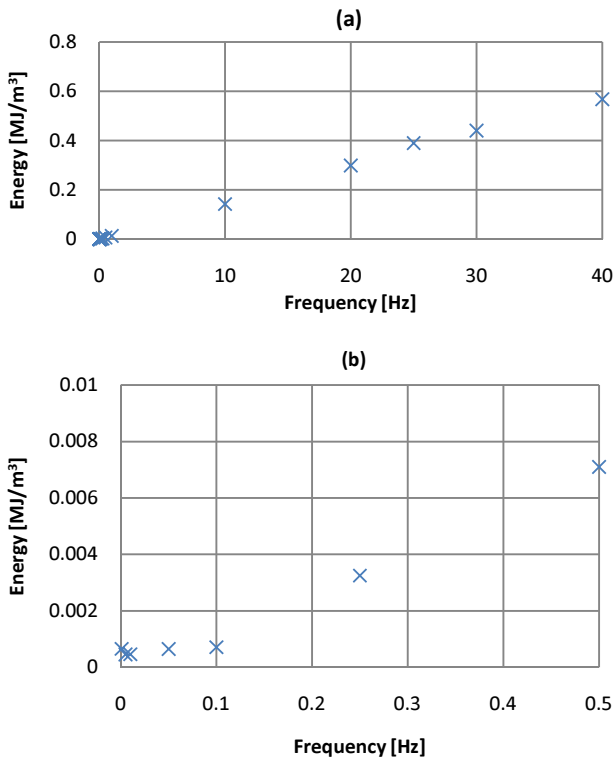


Figure 6. (a) Energy vs Frequency (Range 0-40 Hz)  
(b) Energy vs Frequency (Range 0-0.5 Hz)

Hysteresis data were collected throughout the lifetime of four specimens at four stress levels. For the stress levels of 241 MPa and 259 MPa, hysteresis data were collected for five consecutive cycles at 0.1 Hz with 60 data points per cycle, followed by 95 cycles with no data collection at 10 Hz. Of the five cycles of hysteresis data collected, the 2<sup>nd</sup>, 3<sup>rd</sup> and 4<sup>th</sup> cycles were averaged to represent the strain energy for those 100 cycles (5 cycles at 0.1 Hz and 95 cycles at 10 Hz). This process continued until the specimen fractured. At higher stress levels of 269 MPa and 276 MPa, hysteresis data were collected for every cycle at 0.1 Hz because of the shorter expected lifetime at higher stress levels. For this type of testing, hysteresis data for the five nearest cycles were averaged to represent each data point.

## RESULTS AND DISCUSSION

Monotonic tension tests results are summarized in Table 1. The data was used to calculate the modulus of elasticity, ultimate tensile stress and 0.2% yield stress. The straight line approximation constant for true stress (Equation 3) are also tabulated in Table 1. Figure 7 shows the energy comparison between the two different methods for approximating the post-necking stress-strain behavior during monotonic fracture: the straight line approximation (from Equation 3) and extension of the curve fit equation (Equation 1). Though previous studies used the straight line approximation after necking, comparison of the total energy to fracture using both approximation

methods show the straight line approximation is not necessary. To simplify the method, the single curve fit equation (Equation 1) for monotonic testing may be used with little effect on the fatigue life predictions. For example, in monotonic test #2, the total energy to failure using the straight line approximation is 227.3 MJ/m<sup>3</sup> while the total energy to failure for the curve fit approximation is 232.1 MJ/m<sup>3</sup>.

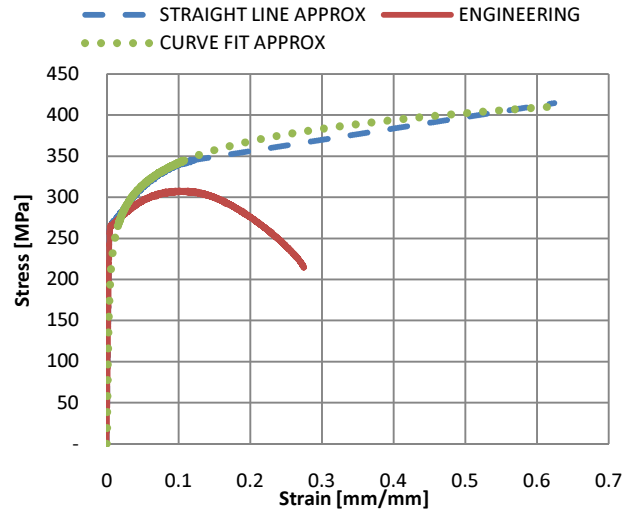


Figure 7. Monotonic test #2 results

Hysteresis data were collected throughout the entire lifetime of the specimen as described in the Experimental Procedures section for four stress levels: 241 MPa, 259 MPa, 269 MPa and 276 MPa. The data were used to determine the amount of strain energy accumulated in each cycle and throughout the specimen's lifetime. The results of these tests are plotted in Figure 8. In order to compare the strain energies at different stress levels, the horizontal axis is plotted as the fraction of the specimen's lifetime. In each case, the strain energy began high and decreased to a steady value before dipping and increasing severely. It should be noted, in each of these tests, the failure crack that eventually completely fractured the specimen formed outside the extensometer gauge length.

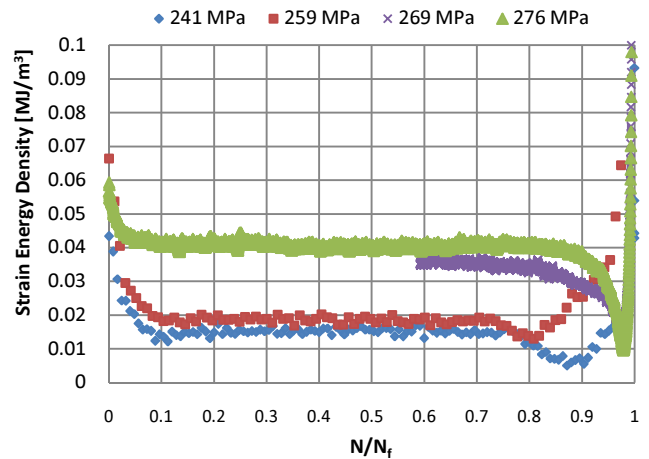


Figure 8. Strain energy throughout lifetime

Table 1. Monotonic Test Results

Test	E (MPa)	$\sigma_n$ (MPa)	$\sigma_y$ (MPa)	$W_{SL}$ (MJ/m <sup>3</sup> )	$W_{CF}$ (MJ/m <sup>3</sup> )	$d_f$ (mm)	$\beta_0$ (MPa)	$\beta_1$ (MPa)
1	70167	324.3	292.3	239.5	247.0	4.636	338.39	31.87
2	68509	308.5	285.1	227.3	232.1	4.648	331.52	39.54
3	69191	316.9	287.4	235.5	245.2	4.737	375.36	32.48
Average	69441	316.57	288.27	233.53	241.43	4.674	348.42	34.63

The underlying assumption of the energy based fatigue lifetime prediction method is that the total energy required to fracture the specimen monotonically should be equal to the cyclic strain energy accumulated throughout the fatigue life of the specimen. Therefore, the total strain energy throughout the lifetime of the specimen was calculated for all the stress values tested based on the continuous hysteresis loop data collection. These results are shown in Table 2.

Table 2. Total energy to failure in fatigue process

Stress Level (MPa)	Energy to failure (MJ/m <sup>3</sup> )
241	211.5
259	216.7
269	225.6
276	207.6

Both the straight line approximation and extended curve fit approximations for the true stress - true strain curve beyond necking were used to determine the expected fatigue life of the specimens. To use the curve fit approximation, a new fatigue life prediction equation must be developed because the equation for calculating total strain energy in a monotonic test is different, see Equation 15. This equation does not use the experimentally determined  $\sigma_n$  or  $\epsilon_n$  nor does it use the curve fit constants  $\beta_0$  and  $\beta_1$ . These results were compared to experimental S-N data points and can be seen in Figure 9. The parameters in Table 3 were used to create the prediction lines in Figure 9.

$$N_f = \frac{\sigma_f \epsilon_f - \frac{\sigma_f^2}{2E} - \epsilon_0 \sigma_0 \left[ \cosh\left(\frac{\sigma_f}{\sigma_0}\right) + 1 \right]}{\frac{2\sigma_c}{c} \left\{ \frac{\sigma_a}{\sigma_c} \sinh\left(\frac{2\sigma_a}{\sigma_c}\right) - \left[ \cosh\left(\frac{2\sigma_a}{\sigma_c}\right) - 1 \right] \right\}} \quad (15)$$

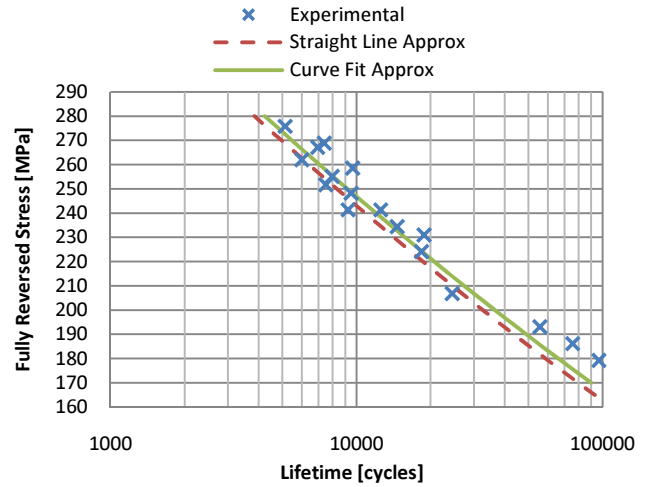


Figure 9. Comparison of fatigue life predictions using both approximations

Table 3. Fatigue prediction parameters

Parameter	Value
$\beta_0$	348.42 [MPa]
$\beta_1$	34.63 [MPa]
$\epsilon_0$	$1.7 \times 10^{-5}$ [mm/mm]
$\epsilon_n$	0.120085 [mm/mm]
$\epsilon_f$	0.61635 [mm/mm]
$\sigma_0$	36.68 MPa
$\sigma_n$	288.27 MPa
$\sigma_c$	100.049 MPa
$\sigma_f$	414.44 MPa
E	69441 MPa
C	1000000
$W_{crit}/W_m$	0.664

In all tests, the strain energy per cycle was constant throughout most of the specimen's lifetime. Near the end of the specimen's lifetime, the strain energy deviates from the constant value. Figure 10 shows the strain energy of these tests near the end of the specimen's lifetime with 5% thresholds around the steady state values for strain energy. The point in the specimen's lifetime when the 5% threshold is crossed is defined as the "critical lifetime." The strain energy accumulated up to the critical point (critical energy) is tabulated in Table 4. The accumulated strain energy to the

threshold crossing point is nearly the same for all stress levels tested. Therefore, it seems that the "critical energy" is a property similar to the failure energy of the specimen.

Table 4. Critical energy in fatigue process

Stress Level (MPa)	Critical Energy (MJ/m <sup>3</sup> )
241	159.4
259	159.7
269	161.7
276	164.6

## CRITICAL LIFE PREDICTION

The critical life of the specimen occurs when the steady state value of cyclic strain energy deviates by 5%. Knowledge of the critical life of a structural component is important because after the critical life, material properties (such as yield stress) begin to change [10]. Four stress levels were tested on Al6061-T6 specimens to determine the cumulative strain energy to the critical life. The cyclic strain energy has been plotted on non-dimensionalized axes in Figure 10. The strain energy has been non-dimensionalized by dividing by the steady state strain energy value for that each particular stress. Figure 10 also shows the 5% threshold limits on the strain energy deviation.

At each stress level the critical energy is nearly equal, thus the "critical energy" is a material property much like the strain energy in a monotonic tension test. Equation 15 is modified to include the critical life prediction by involving the ratio of critical energy to final failure energy. The new failure prediction equation (Equation 15) is multiplied by the ratio of critical energy ( $W_{crit}$ ) to monotonic tension energy ( $W_m$ ). For the case of the Al6061-T6 specimens tested in this study, the critical energy is about 160 MJ/m<sup>3</sup> while the monotonic energy is about 241 MPa, resulting in a ratio of about 66.4%. Equation 16 is the new critical life prediction equation. Using the same parameters as the previous section (Table 3), a critical life prediction is made in Figure 11.

$$N_c = \left( \frac{W_{crit}}{W_m} \right) \frac{\sigma_f \varepsilon_f - \frac{\sigma_f^2}{2E} - \varepsilon_0 \sigma_0 \left[ \cosh\left(\frac{\sigma_f}{\sigma_0}\right) + 1 \right]}{\frac{2\sigma_c(\sigma_a)}{c} \sinh\left(\frac{2\sigma_a}{\sigma_c}\right) - \left[ \cosh\left(\frac{2\sigma_a}{\sigma_c}\right) - 1 \right]} \quad (16)$$

The energy based fatigue prediction framework accurately predicts the fatigue life of the specimens. The prediction often goes through the scattered points, which give a good estimation of the expected cycles to failure. The critical life prediction line in Figure 11 accurately sets a lower limit for the expected lifetime of specimens - all of the specimens tested in this study had longer fatigue lifetimes than the critical life prediction.

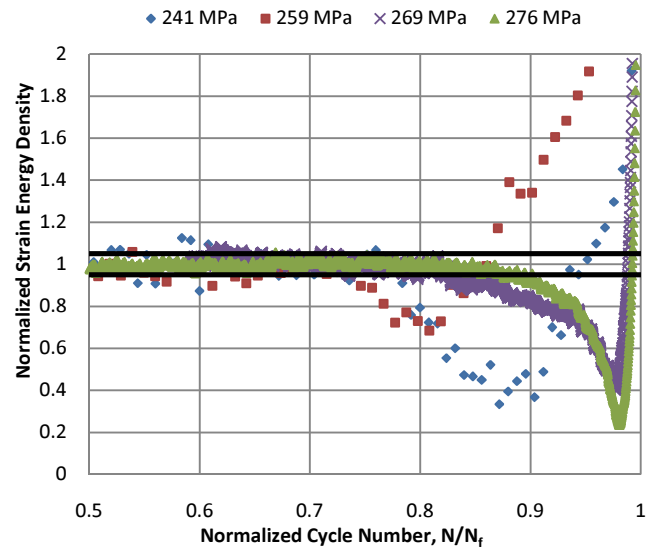


Figure 10. Critical energy threshold

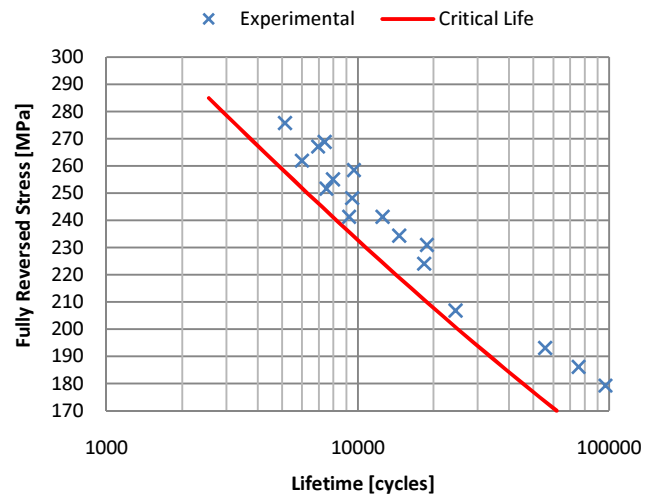


Figure 11. Critical life prediction

## CONCLUSIONS

The energy based framework for predicting fatigue failure has been simplified by modifying the true stress - true strain approximation beyond necking which reduces the number of necessary parameters by four. A material property, critical energy, has been found to obtain a "critical lifetime" prediction. The critical lifetime predicts the point in the specimen's lifetime when its behavior changes. At this point in the specimen's lifetime, material properties such as yield strength change. The critical lifetime estimate also seems to provide a safe limit for all S-N data points. In real world structural components, the useful life of the component will have ended at the critical lifetime and the component should be replaced to maintain a failure free system. The discovery of the critical energy will aid in reducing the number of unexpected fatigue failures and may also lead to advances in structural health monitoring.

## ACKNOWLEDGMENTS

The authors would like to thank the Air Force Research Laboratories (AFRL), specifically the Turbine Engine Fatigue Facility (TEFF), for the use of their facilities and equipment.

## REFERENCES

- [1] George, T., Siedt, J., Shen, M.-H. H., Cross, C., and Nicholas, T., "Development of a Novel Vibration-Based Fatigue Testing Methodology," *International Journal of Fatigue* 2004; Vol 26, pp 477-486.
- [2] Goodman, J., 1899, *Mechanics Applied to Engineering*, Longmans, Green, and Co., London.
- [3] Nicholas, T., "Critical Issues in High Cycle Fatigue," *International Journal of Fatigue*, 1999; 21:S221-S231.
- [4] Jasper, TM, "The Value of the Energy Relation in the Testing of Ferrous Metals at Varying Ranges of Stress and at Intermediate and High Temperatures," *Philosophical Magazine Series*. 6, Oct. 1923; 46: pp. 609-627
- [5] Enomoto, N., "On fatigue tests under progressive stress. Proc ASTM 55, pp. 903-917, 1965.
- [6] Stowell, E., "A study of the energy criterion for fatigue," *Nuclear Engineering and Design*, 3, pp 32-40, 1966.
- [7] Scott-Emuakpor, O., Shen, M-HH, George, T., Cross, C., "An Energy-Based Uniaxial Fatigue Life Prediction Method for Commonly Used Gas Turbine Engines Materials," *ASME Journal of Engineering for Gas Turbines and Power*, Vol 130, November 2008, pp 1-15.
- [8] Scott-Emuakpor, O., Shen, M-HH, George, T., Cross, C., "Multi-Axial fatigue-life prediction via a strain-energy method." *AIAA Journal*, Vol 48, Number 1, January 2010.
- [9] Feltner, C.E., and Morrow, J.D., "Microplastic Strain hysteresis Energy as a Criterion for Fatigue Fracture," *Journal of Basic Engineering Transactions, American Society of Mechanical Engineers*, New York, 1961, Vol. 83, pp. 15-22.
- [10] Ozaltun, H., Shen, M-MH, George, T., Cross, C. "An Energy Based Fatigue Life Prediction Framework for In-Service Structural Components". *Journal of Experimental Mechanics*, DOI: 10.1007/s11340-010-9365-z
- [11] Wertz, J., Shen, M-H., George, T., Cross, C., Scott-Emuakpor, E. "An Energy-based Torsional Fatigue Life-Prediction Method". *ASME/IGTI Turbo Expo*, 2010; GT2010-22647
- [12] Panontin, T., and Sheppard, S., "Fatigue and Fracture Mechanics," *ASTM, STP-1332*, 1999; Vol. 29, ASTM International, West Conshohocken, PA.
- [13] Chang, C.S., Pimbley, W.T., Conway, H.D., "An analysis of metal fatigue based on hysteresis energy." *Journal of Experimental Mechanics* 8(3), pp. 133-137, 1968.
- [14] MayerCampbell Laird, H., "Frequency effects on cyclic plastic strain of polycrystalline copper under variable loading," *Material Science and Engineering A*, Vol 194, Issue 2, pp. 137-145, May 1995.
- [15] Scott-Emuakpor, O., George, T., Cross, C., and Shen, M.-H.H., "Hysteresis Loop Representation for Strain Energy Calculation and Fatigue Assessment," *Journal of Strain Analysis for Engineering Design*, 2010, Vol. 45, Issue 4, pp. 275-282.
- [16] Zhang, J., Jiang, Z. "An experimental study of inhomogeneous cyclic plastic deformation of 1045 steel under multiaxial cyclic loading," *International Journal of Plasticity*, Vol 21, Issue 11, pp. 2174-2190, November 2005.
- [17] American Society of Test and Materials, ASTM E466: Standard Practice for Conducting Force Controlled Constant Amplitude Axial Fatigue Tests of Metallic Materials 03.01, 2007.
- [18] Aerospace Material Specifications, SAE AMS 2772-E: heat treatment of aluminum alloy raw materials, 2008.
- [19] American Society for test and materials, ASTM B211-03-M: standard specification for aluminum and aluminum -alloy bar rod and wire, book of standards, volume: 02.02, 2008.
- [20] American Society for Test and Materials ASTM E8/E8M-08: standard test methods for tension testing of metallic materials, book of standards, volume: 03.01, 2008.
- [21] MTS TestStar IIs Software Manual